The International Supercritical CO_2 Energy Technologies Symposium
March 2 - 5, 2026, Pittsburgh, PA
Paper #

INVESTIGATION OF IGNITION AND STABILIZATION OF CO2-DILUTED METHANE-OXYGEN FLAME ABOVE CARBON DIOXIDE CRITICAL PRESSURE

Francesco Di Sabatino **Austin Jones** **Mariana Rodriguez Chavez** **Brynn Bartholomew** **Seokwon Cho** **Seth Cunningham** **Steve White**
Southwest Research Institute, San Antonio, TX, U.S.A.

Akihiko Miyahara **Yohei Mikami** **Naohide Higuchi**
Mitsui Energy Development CO., LTD, Tokyo, Japan

ABSTRACT

Direct-fired oxy-fuel supercritical CO_2 (sCO_2) power cycles present an innovative approach to significantly reduce or potentially eliminate carbon emissions from hydrocarbon fuel combustion. However, the operating conditions of these systems—marked by extreme pressures, high temperatures, and substantial CO_2 dilution—pose unique challenges for flame stabilization. This study investigates oxy-fuel combustion under relevant operating conditions to explore flame stabilization and ignition mechanisms in CO_2-diluted environments. Laser ignition and flame stabilization were experimentally investigated in oxygen/methane-fired combustors under various thermodynamic conditions and CO_2-dilution levels, which included both subcritical and supercritical CO_2 pressures. A simplified test rig was designed to mimic a realistic combustor geometry and to provide optical access for a detailed examination of the combustion and ignition processes. The results indicated that both pressure and CO_2 dilution have a strong influence on the ignition characteristics and flame stability, providing useful insights for future developments in this field.

INTRODUCTION

Direct-fired oxy-fuel supercritical carbon dioxide (sCO_2) power cycles offer a promising route to achieve near-total carbon capture while continuing to utilize existing fossil fuel resources. In these power cycles, supercritical CO_2 acts as the working fluid, with oxygen and fuel directly introduced into a combustor to drive the combustion process [1]. The complete combustion of methane (CH_4) and oxygen (O_2) produces carbon dioxide (CO_2) and water (H_2O). Since the CO_2 generated during combustion remains within a closed-loop system, the surplus CO_2 can be easily extracted at the low-temperature section of the cycle, enabling effective carbon capture and sequestration. Additionally, utilizing direct-firing—where the fuel is burned directly within the working fluid—eliminates energy losses associated with heat exchangers (a characteristic of indirect firing), thereby improving the overall efficiency of the cycle [1].
The combination of high efficiency and the ability to achieve near-100% carbon capture makes this technology an appealing candidate for future base-load power generation. However, leveraging the advantageous properties of sCO_2 requires that some or all of the thermodynamic cycle conditions exceed CO_2's critical point: 31.0 °C and 73.8 bar [2]. While achieving this temperature is relatively straightforward, the high pressure required is significantly greater than that of traditional gas turbine combustors, resembling more operating conditions in rocket engines [3].

Despite the strong potential of direct-fired oxy-fuel combustion, the operational characteristics of CO_2 combustors remain poorly understood. While several computational studies and limited experimental data have provided valuable insights [4]-[23], substantial knowledge gaps remain. Strakey *et al.* [7] introduced key computational challenges associated with this technology, while White *et al*. [8] studied design-related difficulties in combustor development. Banuti *et al.* [9] conducted a detailed computational study, emphasizing the complexities of fuel and oxidizer mixing as well as combustion dynamics in a conceptual combustor geometry. Cecere *et al.* [10] performed direct numerical simulations (DNS) of a CO_2-diluted CH_4/O_2 flame produced by a slot burner at conditions relevant to sCO_2 power cycles, revealing that density-gradient-induced stratified flow fields can hinder CO_2 dilution in the flame zone. Experimental advancements include the work of Suzuki et al. [12], who successfully demonstrated the operation of an entire 50 MW direct-fired oxy-fuel sCO_2 cycle; however, detailed combustor-level data from this study remain unavailable. Therefore, additional open test data would be useful to those designing and building these power cycles. Lee *et al.* [22] experimentally examined the stabilization of CO_2-diluted CH_4/O_2 jet flames, while Yang *et al.* [15], Bukar *et al.* [13], [14], and Di Sabatino et al. [23] performed similar investigations. Kutne *et al.* [16] studied the stability of CO_2-diluted CH_4/O_2 swirl flames. However, these experimental efforts were conducted at pressures well below CO_2's critical pressure.

Our current understanding reveals a substantial lack of experimental data at operating conditions corresponding to pressures above the critical point of CO_2. To the best of the authors' knowledge, no studies in the literature investigate the combustion behavior of CO_2-diluted fuel mixtures at conditions directly relevant to direct-fired power cycles. Thus, the present study aims to examine ignition characteristics and pressure effects on CO_2-diluted methane flames, spanning operating conditions below and above the critical point of CO_2. This represents the first investigation of this nature and constitutes a significant advancement in understanding operational combustion processes for direct-fired oxy-fuel sCO_2 power cycles. It is important to note that, due to client confidentiality, all data presented in this paper has been normalized, and only trends are discussed. Furthermore, detailed geometric and performance information about the test rig and instrumentation have been omitted for the same reason.

EXPERIMENTAL SETUP AND PROCEDURE

The following section outlines the experimental setup and procedure used for data collection and analysis in this study. It begins with descriptions of the nozzle geometry, pressure vessel, laser ignition system, and optical diagnostics. Subsequently, the experimental procedure and the operating conditions examined are detailed.

Experimental setup and optical diagnostics

The experimental setup utilized in this work is depicted in Figure 1. Fuel, oxidizer, and co-flow streams were injected into the pressure vessel using a concentric circular nozzle configuration, The fuel mixture was injected through the central tube, while the oxidizer mixture was introduced through the annular region surrounding the fuel tube. The co-flow, composed entirely of CO_2, was injected into the outer annular region via a flow straightener to ensure uniform flow. The exit cross-sectional areas of the three nozzles were carefully aligned to ensure that mixing occurred only within the pressure vessel. This nozzle assembly was mounted within a cylindrical pressure vessel capable of withstanding the extremely high pressures and temperatures associated with the oxy-fuel combustion process in the sCO_2 system. To precisely control operating pressure, a diaphragm-based back-pressure regulator (Equilibar EQ-20669), not shown in Figure 1, was installed downstream of the pressure vessel. The co-flow stream served a dual purpose: thermally protecting the pressure vessel walls and aiding in pressure stabilization within the system. Additionally, an internal water-cooling system continuously circulated water through passages within the pressure vessel to enhance heat dissipation. The vessel was equipped with optical access for observing and investigating the combustion process and ignition. Two large rectangular sapphire windows were installed for flame visualization, while a smaller sapphire window was dedicated to laser ignition.

Ignition was consistently achieved using a laser-based system. A 10 Hz Nd:YAG laser (Quantel Qsmart Twins) was implemented to generate the 532-nm laser beam with a theoretical energy per pulse of 430 mJ. A 6 ns laser pulse was used. The beam was directed to the pressure vessel using a series of compatible mirrors and focused few centimeters above the fuel nozzle exit cross-section area, using a plano-convex lens.

Flow rates for oxygen, methane, and CO_2 were precisely controlled using stem valves (LowFlow precision control valves) and measured using differential pressure sensors (Rosemount W/305RC32B11) in conjunction with orifices (Brice Barclay), thermocouples, and static pressure sensors. Three separate CO_2 lines were used: one dedicated to controlling the co-flow, and two others for managing the flow rates of CO_2 mixed with the oxidizer and fuel streams. To ensure that all CO_2 streams entered the pressure vessel above the critical temperature, two large electric heaters (Gaumer Process) were installed upstream of the stem valves and downstream of the orifices. Furthermore, all CO_2 lines were thermally insulated and equipped with external tube heaters to maintain temperatures above the critical threshold.

Several high-temperature type K thermocouples (Omega KQXL-116U-12-ROHS) were installed longitudinally and radially along the combustor to monitor the temperature distribution within the pressure vessel. Static pressure was measured using a high-accuracy static pressure sensor (Omega PX409-1.5KAI), while dynamic pressure variations, including the pressure rise at ignition and potential combustion instabilities, were monitored using dynamic pressure transducers (PCB 1860). All sensors were mounted with extended standoffs to ensure sufficient separation from the hot combustion gases, maintaining their safe operating temperatures. Flame visualization was conducted using two CCD cameras (Basler aca1920 50 GC) positioned to capture natural luminosity through the two large rectangular sapphire windows. These cameras were used to monitor flame behavior, including ignition and combustion characteristics.

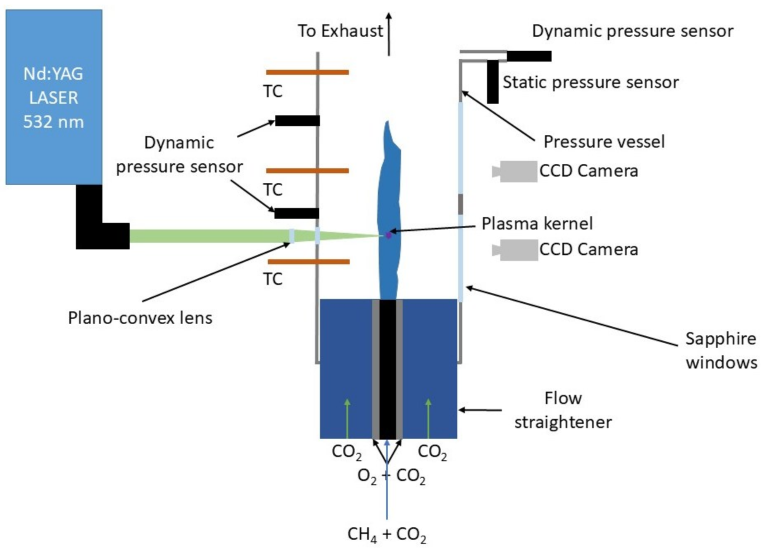

FIGURE 1: SCHEMATIC OF THE EXPERIMENTAL SETUP. DIMENSIONS ARE NOT AT SCALE.

Experimental procedure and operating conditions

Two series of experiments were conducted for this study. The first series focused on evaluating ignition propensity as a function of pressure, while the second series investigated the effects of pressure on the combustion process. Both series followed a similar ignition procedure. CO_2 streams were maintained for the entire duration of the test. The flow rates of oxygen, methane, and CO_2 were carefully set to achieve the desired flame thermal power and static pressure before initiating the laser ignition system and generating the ignition kernel. To reach the required static pressure in the vessel, adjustments were made to the opening of the backpressure regulator. Therefore, methane flow was stopped, while CO_2 and O_2 flows were maintained to sustain the target static pressure. The laser system was then activated, and ignition kernel formation was confirmed using the lower CCD camera. Data acquisition commenced only if the ignition kernel was successfully and consistently formed, after which the methane flow was restored. This procedure was designed to prevent the pressure vessel from becoming saturated with methane, thereby ensuring safety and improving reliability. If ignition was not achieved within 10 seconds, methane flow and the laser system were deactivated. Upon successful ignition and flame stabilization, the laser system was turned off. Steady-state combustion was confirmed using a constant temperature profile measured by thermocouples installed downstream of the flame. For the second series of tests, pressure within the system was incrementally increased after achieving steady-state combustion from ignition conditions to values above the critical pressure of CO_2, in steps designed to minimize flame disturbances.

In this series of tests, the mole fraction of CO_2 in the fuel stream was also increased to assess blow-off limits at relevant operating conditions. To maintain a balanced overall composition, the mass flow rate of CO_2 in the oxidizer stream was reduced proportionately to the increase in CO_2 mole fraction in the fuel stream. Note that the flow rates of all fluids injected into the combustor were deliberately scaled with pressure to maintain nearly the same nozzle exit velocity as pressure increased

During both experimental series, data were collected for 30 seconds at steady-state conditions for each operating point. Flame natural luminosity images were recorded at an average framerate of 100 frames per second (fps), yielding approximately 1,000 images per operating condition. Temperature and static pressure data along the pressure vessel were recorded at one data point per second, while dynamic pressure data were collected at 10 kHz. Once data collection was completed, the flame was extinguished by stopping the methane flow, while the CO_2 flows were maintained to cool and purge the pressure vessel. To ensure reproducibility, this procedure was repeated multiple times at each operating condition.

All measured temperature, pressure, and flow rate data were averaged over the 30-second data collection period. The peak pressure during ignition was determined by analyzing the dynamic pressure sensor data, with the peak recorded immediately following ignition. Flame natural luminosity images were pre-processed by summing individual frames to create an average image, which was subsequently corrected for background noise. To characterize the flame length, a binarization procedure based on Otsu's method [24], was applied, followed by noise reduction using a median filter. The flame length was measured as the distance between the base and the tip of the flame. Due to experimental limitations, significant uncertainty in the flame length data was observed; therefore, only general trends of flame length as a function of pressure are discussed in this paper. An example of the flame image processing technique is presented in Figure 2. All data presented in this study have been normalized to their respective maximum values

The first series of experiments was limited to operating conditions below the critical pressure of CO_2. Higher pressures were not tested in this series due to unreliable ignition observed under those conditions. In contrast, the second series of experiments included tests at both subcritical and supercritical pressure levels of CO_2. The operating conditions for these experiments, including the overall CO_2 mole fraction and equivalence ratio, closely resembled those used in a direct fired cycle. However, the CO_2 mole fraction in the oxidizer stream was slightly lower than typically applied in such cycles. Due to client confidentiality, further details regarding specific operating conditions cannot be disclosed, as previously noted.

RESULTS AND DISCUSSION

The data collected in this work and the corresponding analysis are presented in this section. First, data relating to ignition, including equivalence ratio, CO_2 mole fraction, and peak pressure are shown and discussed. Thereafter, the results related to pressure effects and blow-off are presented and analyzed.

Ignition results and analysis

Figure 3 presents a summary of the ignition tests, plotting normalized pressure against the normalized equivalence ratio. Successful ignition events are represented by black circles, while failed attempts are denoted by red crosses. Note that the equivalence ratio has also been normalized relative to its maximum value. The figure demonstrates that ignition was predominantly successful at equivalence ratios relevant to direct power cycles. The failed ignition events at equivalence ratios substantially deviating from the ideal value are likely attributable to reduced reactivity, which may have been caused by either insufficient fuel or oxidizer mass flow rates. However, ignition failures occurring at equivalence ratios near the ideal value warrant further investigation to identify potential underlying causes. As evident from Figure 3, ignition at pressures approaching the critical pressure of CO_2 was successfully achieved without causing damage to the system or adversely affecting the stability of the generated flame. This suggests that the system can operate reliably under these extreme conditions, offering promising results for direct fired oxy-fuel sCO_2 power cycles.

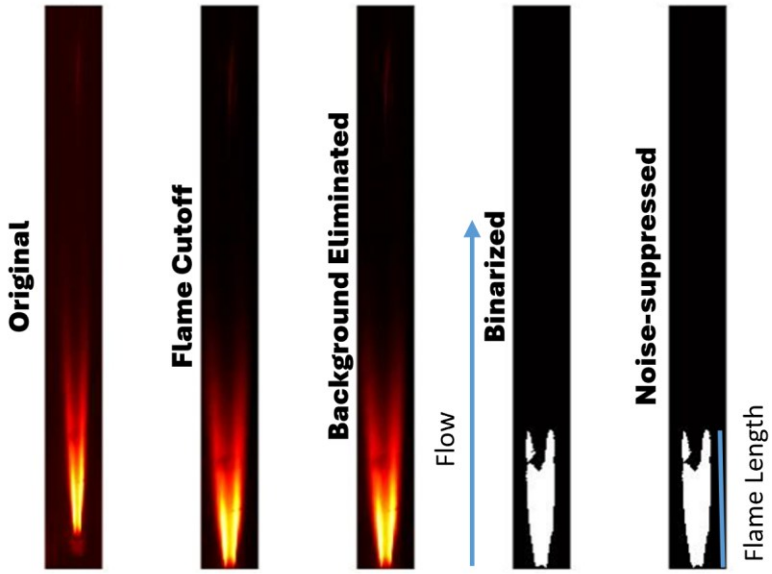

FIGURE 2: EXAMPLE OF FLAME IMAGE PROCESSING

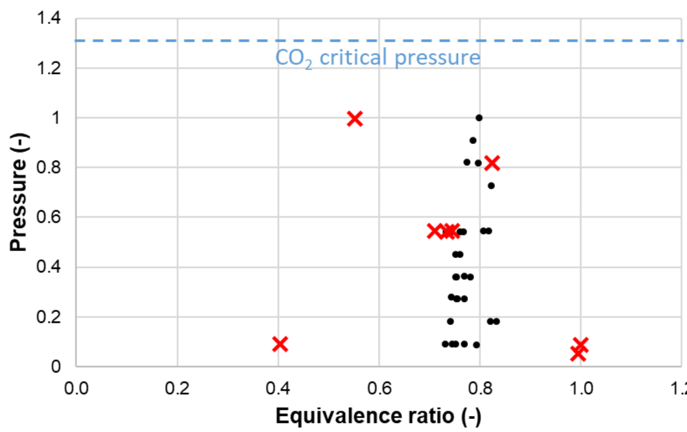

FIGURE 3: NORMALIZED PRESSURE AT IGNITION VS EQUIVALENCE RATIO. THE CRITICAL PRESSURE OF CO_2 IS HIGHLIGHTED.

Figure 4 shows the normalized mole fraction of CO_2 in the oxidizer (top) and fuel streams (bottom) at ignition. Similar to Figure 3, successful ignitions are marked by black circles, while failures are indicated by red crosses. Since crosses and circles are well mixed together, it is reasonable to assume that CO_2 mole fraction in the oxidizer stream has a limited impact on ignition. However, over 50% of the failures occur above 0.6 of normalized mole fraction of CO_2 in the fuel stream. Thus, a high concentration of CO_2 in the fuel stream appears to be a contributing factor to failed ignition events. Note that a high CO_2 concentration in the fuel stream also results in higher velocity and density at the nozzle exit, potentially affecting the mixing between fuel and oxidizer and, consequently, ignition propensity. Overall, 0.6 and below normalized mole fraction of CO_2 in the fuel stream resulted in repeatable ignition. Overall, three phenomena are thought to contribute to ignition failures:

- Too low or high equivalence ratio, reducing mixture reactivity
- Elevated CO_2 mole fraction in the fuel stream, diminishing mixture reactivity
- Elevated CO_2 mole fraction in the fuel stream, increasing fuel velocity and density at the nozzle exit and impairing the mixing process between fuel and oxidizer

Note that additional analysis should be performed to verify this hypothesis. Due to project limitation, this was not possible during this work.

An increase in pressure was observed following an ignition event due to the confined nature of the system. The peak pressure increases as a function of system pressure is shown in Figure 5. It is noteworthy that the peak value is quite reproducible between different ignition events for pressures up to 0.6. However, from 0.6 to 1, the values became more variable, possibly indicating a more stochastic post-ignition phase. Throughout the analyzed operating conditions, this pressure peak consistently remained around a maximum of 1% of the system pressure.

1.2 Pressure effects and blow-off results and analysis

Figure 6 illustrates changes in processed flame length as a function of combustor pressure while maintaining a constant mole fraction of CO_2 in the fuel and oxidizer streams. The pressure data is normalized using the same pressure value as in Figures 4 and 5 to facilitate direct comparison. Additional data were collected at pressure above the critical point, but they are not presented in Figure 6 since they were gathered at different mole fraction values of CO_2 in the fuel and oxidizer streams. The results suggest that flame length is not significantly influenced by pressure under these specific conditions. As noted previously, fluid flow rates were carefully scaled with pressure to maintain approximately the same nozzle exit velocity. This adjustment likely mitigated the influence of pressure on flame length.

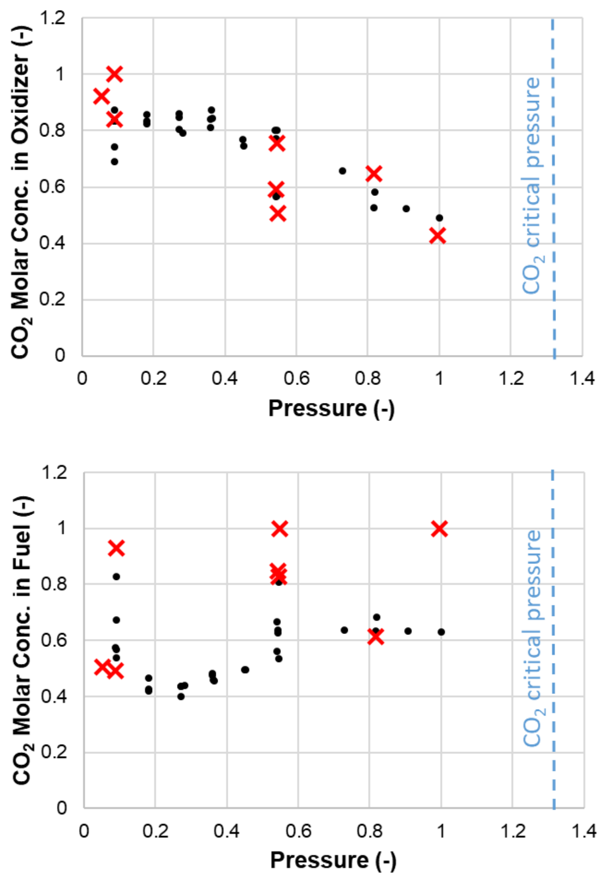

FIGURE 4: NORMALIZED MOLE FRACTION OF CO_2 IN THE OXIDIZER (TOP) AND FUEL (BOTTOM) STREAMS AT IGNITION VS PRESSURE. THE CRITICAL PRESSURE OF CO_2 IS HIGHLIGHTED.

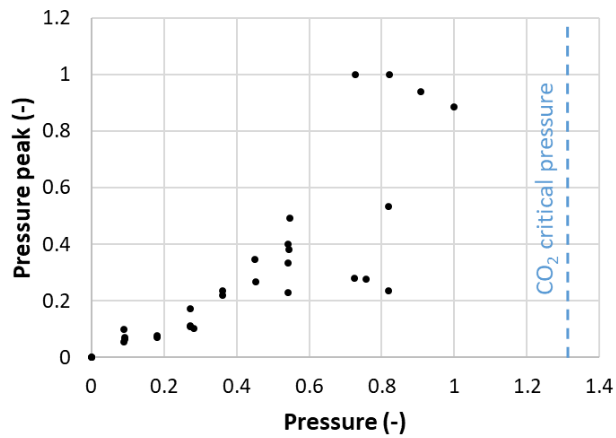

FIGURE 5: NORMALIZED PEAK PRESSURE AT IGNITION VS PRESSURE. THE CRITICAL PRESSURE OF CO_2 IS HIGHLIGHTED.

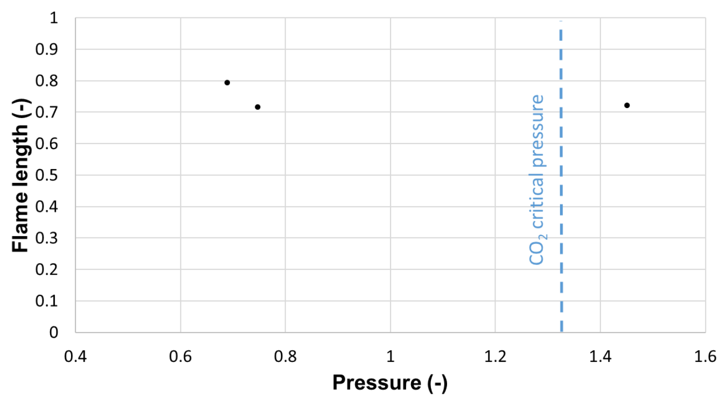

FIGURE 6: NORMALIZED FLAME LENGTH VS PRESSURE. THE CRITICAL PRESSURE OF CO_2 IS HIGHLIGHTED.

At the highest tested pressure, the mole fraction of CO_2 in both the oxidizer and fuel streams was modified to assess its impact on flame length. Figure 7 shows normalized flame length data against normalized mole fraction of CO_2 in fuel (top) and oxidizer (bottom), respectively, at maximum pressure condition, above the critical point. The flame length was shown to decrease with higher CO_2 mole fractions in the fuel stream, which corresponded with reduced CO_2 mole fractions in the oxidizer stream. As mentioned earlier, when the CO_2 mole fraction in the fuel stream increased, the corresponding mass flow rate of CO_2 also increased. To balance this change, the mass flow rate, and thus the mole fraction, of CO_2 in the oxidizer stream was reduced by the same amount. With the current dataset, it is not possible to determine whether the fuel or oxidizer CO_2 mole fraction has the larger impact on flame length at constant pressure. Additional analyses are required to investigate this trend thoroughly.

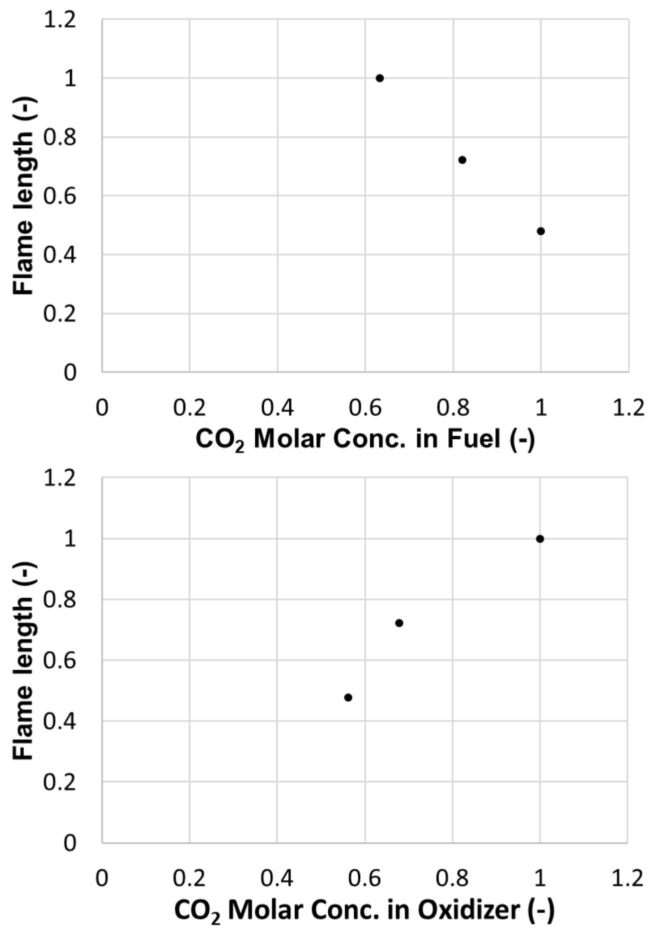

FIGURE 7: NORMALIZED FLAME LENGTH VS MOLE FRACTION OF CO_2 IN THE OXIDIZER (TOP) AND FUEL (BOTTOM) STREAMS ABOVE THE CRITICAL PRESSURE.

A series of tests was performed to evaluate flame blow-off limits under varying pressure conditions and CO_2 mole fractions in the fuel stream. Once the target combustor pressure was reached, the CO_2 mole fraction in the fuel stream was incrementally increased from its initial value until blow-off occurred. Following a methodology similar to that of Lee *et al.* [22], Figure 8 depicts the relationship between the Reynolds number (Re) at the fuel nozzle exit and the normalized CO_2 mole fraction in the fuel stream under maximum pressure conditions, which were well above the critical pressure of CO_2. The linear trend observed between these two parameters is expected due to the simultaneous increase in fuel density and exit velocity as the CO_2 mole fraction rises. However, this figure provides limited insight into the blow-off phenomenon. Figure 9 presents the normalized CO_2 mole fraction in the fuel stream as a function of the velocity ratio between the fuel and oxidizer nozzle exit velocities under the same conditions as Figure 8.

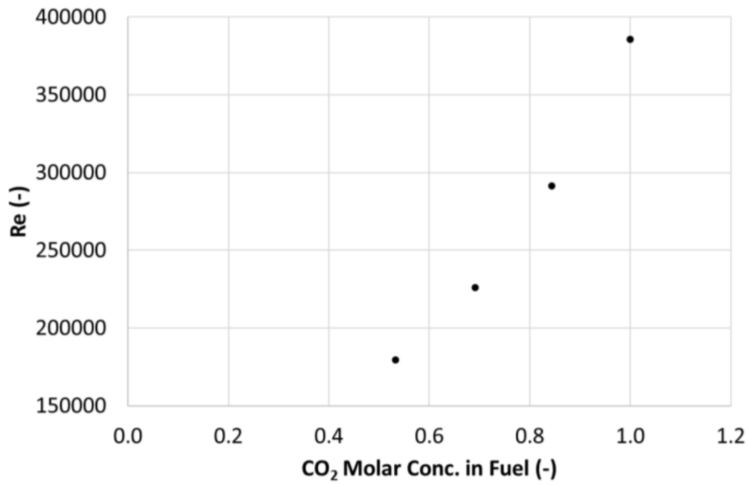

FIGURE 8: REYNOLD NUMBER VS NORMALIZED MOLE FRACTION OF CO_2 IN THE FUEL STREAM ABOVE THE CRITICAL PRESSURE.

While Figure 9 provides insights specific to the highest pressure analyzed, similar trends were observed for other pressure conditions. The linear increase in CO_2 mole fraction with the velocity ratio suggests the interaction of two phenomena. First, the higher CO_2 mole fraction in the fuel stream increases both the fuel nozzle exit velocity and the velocity ratio as well as density, affecting the mixing field between the fuel and oxidizer streams. Second, the higher CO_2 mole fraction reduces mixture reactivity, impacting the combustion process. To explore these interactions, Figure 10 compares results for two different fuel nozzle diameters at a lower operating pressure than those used in Figure 9, as similar comparisons could not be performed under the highest operating pressure. The larger-diameter nozzle (Nozzle 2) exhibited higher CO_2 mole fractions at equivalent velocity ratios, emphasizing the role of the fuel/oxidizer mixing field farther from the blow-off limit. However, near the blow-off limit, the results for both nozzles showed similar CO_2 mole fraction for different velocity ratio, suggesting that mixture reactivity, rather than velocity ratio, may dominate the blow-off phenomenon. Additional experiments are required to further understand these interactions and assess the predominant mechanism near the blow-off limit.

Temperature measured at the exhaust section of the system was also investigated during the blow-off tests. The normalized results for the highest pressure condition investigated in this study are shown in Figure 11, with the mole fraction of CO_2 in the fuel normalized using the same reference as in Figure 8 for consistency.

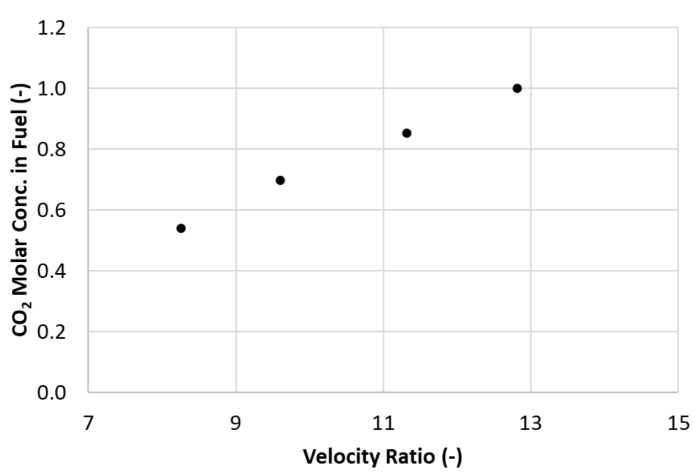

FIGURE 9: NORMALIZED MOLE FRACTION OF CO_2 IN THE FUEL STREAM VS RATIO OF FUEL NOZZLE EXIT VELOCITY TO OXIDIZER NOZZLE EXIT VELOCITY.

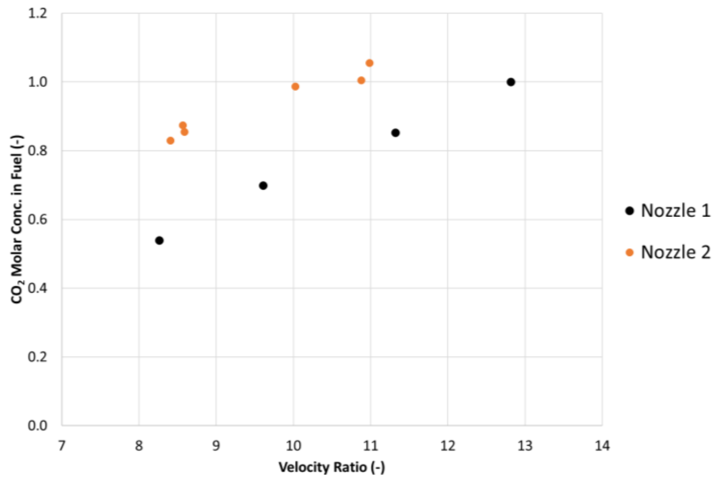

FIGURE 10: NORMALIZED MOLE FRACTION OF CO_2 IN THE FUEL STREAM VS RATIO OF FUEL NOZZLE EXIT VELOCITY TO OXIDIZER NOZZLE EXIT VELOCITY FOR TWO DIFFERENT FUEL NOZZLE DIAMETERS.

A non-linear decrease in exhaust temperature was observed with increasing CO_2 mole fraction in the fuel stream, potentially reflecting reduced mixture reactivity caused by higher CO_2 dilution. However, the temperature differences were modest, preventing definitive conclusions. This subtle difference could be generated from the presence of the co-flow, which may homogenize the temperature across operating conditions. Additional tests are necessary to better understand the relationship between exhaust temperature, CO_2 mole fraction, and reactivity.

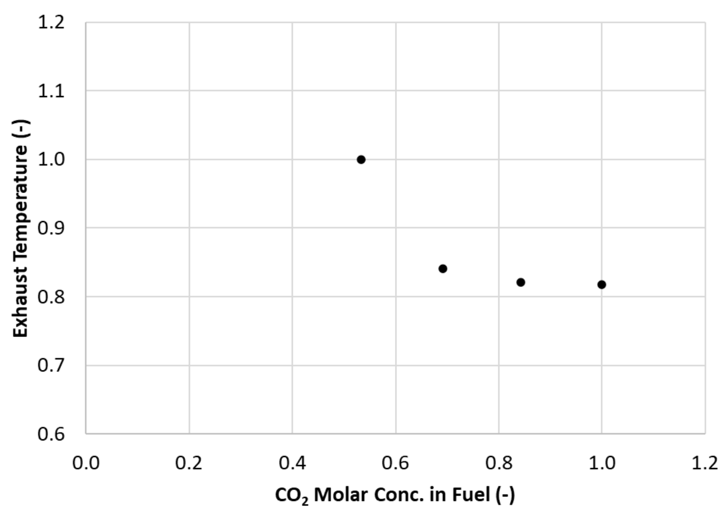

FIGURE 11: NORMALIZED EXHAUST TEMPERATURE VS MOLE FRACTION OF CO_2 IN THE FUEL STREAM

CONCLUSIONS

A system to investigate CO_2-diluted methane-oxygen flames above CO_2 critical pressure has been developed. Ignition and blow-off limits have been investigated using natural luminosity imaging as well as temperature and pressure sensors. A concentric nozzle configuration has been implemented with flow rates of the various fluids being selected to closely represent operating conditions of a real direct fired power cycle. Operating conditions spanned a range of pressure below and above the critical point of CO_2. All data presented in the paper have been normalized to preserve client confidentiality. The main findings of this study are:

- Successful ignition has been generally achieved for equivalence ratios close to the ideal operating conditions for a direct fired cycle. However, failures were observed when equivalence ratios deviated significantly from the optimum range. Elevated CO_2 mole fractions in the fuel stream were identified as a contributing factor to ignition failures, likely due to reduced mixture reactivity and higher nozzle exit velocities as well as densities that impair fuel-oxidizer mixing. Ignition was repeatable and reliable when the normalized CO_2 mole fraction in the fuel stream was ≤0.6. Notably, ignition at pressures near the critical pressure of CO_2 was achieved without any visible system damage or negative effects on the flame, demonstrating the feasibility of operating under such high-pressure conditions.
- Peak pressures after ignition were highly reproducible up to normalized system pressures of 0.6, but became stochastic above this range. Importantly, the peak value consistently remained within 1% of the system pressure, ensuring operational safety under all tested conditions.
- The normalized flame length remained largely unaffected by pressure changes over the tested range, likely due to the deliberate scaling of fluid flow rates to maintain nearly constant nozzle exit velocity. At maximum system pressure, increasing the CO_2 mole fraction in the fuel stream resulted in a reduction in flame length, while a simultaneous decrease in CO_2 mole fraction in the oxidizer stream complicated the identification of which parameter had the dominant effect. Further tests are needed to investigate these interacting variables.
- Blow-off limits were investigated as a function of CO_2 mole fraction in the fuel stream, nozzle exit velocity ratios, and nozzle geometry. Increasing the CO_2 mole fraction in the fuel stream led to higher nozzle exit velocities and velocity ratios as well as densities, highlighting the impact of CO_2 on both mixing dynamics and mixture reactivity. At near blow-off conditions, the observed similarity in blow-off limits between two different nozzle diameters suggests that reduced mixture reactivity, rather than mixing, may be the dominant mechanism. However, further experimental data are needed to confirm this hypothesis, especially at higher operating pressures.
- Exhaust temperatures decreased non-linearly with increasing CO_2 mole fraction, consistent with reduced reactivity of the combustion mixture. Despite this trend, the overall temperature differences were relatively small, potentially due to the homogenizing effect of the co-flow, limiting definitive conclusions.

This work offers an initial understanding of the role of CO_2 dilution and pressure on ignition and flame stability in a high-pressure sCO_2 oxy-methane combustion system. While valuable insights have been gained, critical limitations, including the inability to fully decouple mixing and reactivity effects, highlight the need for additional investigations. The findings provide foundational knowledge for the development of safe and sCO_2 oxy-methane combustion system, particularly for direct fired cycle applications, where CO_2 dilution and high-pressure operation are key design considerations. Additionally, ignition and stabilization of flames with high level of CO_2 dilution in the fuel stream at relevant operating conditions has been demonstrated for the first time, to the best of authors' knowledge.

REFERENCES

[1] K. Brun, P. Friedman, and R. Dennis, *Fundamentals and applications of supercritical carbon dioxide (sCO2) based power cycles*. Woodhead publishing, 2017. Accessed: Jan. 11, 2024. [Online]. Available: https://books.google.com/books?hl=en&lr=&id=o-HxDAAAQBAJ&oi=fnd&pg=PP1&dq=book+supercritical+CO2+combustion+book&ots=L-J59IRLZd&sig=LjaIg-U-zzVYB9QKFvfDRZwB4gk

[2] "NIST Chemistry WebBook." [Online]. Available: https://webbook.nist.gov/chemistry/

[3] A. H. Lefebvre, "Gas Turbine," *Combustion*, 1999, Accessed: Jan. 11, 2024. [Online]. Available: https://www.academia.edu/download/60957118/Gas_Turbine_combustion_Arthur20191020-125598-2chndy.pdf

[4] K. M. Katcher, T. C. Allison, S. Coogan, Y. Jin, C. Lim, and S. Chang, "Igniter Testing for sCO2 Oxy-Combustion," in *Turbo Expo: Power for Land, Sea, and Air*, American Society of Mechanical Engineers, 2019, p. V009T38A017. Accessed: Jan. 11, 2024. [Online]. Available: https://asmedigitalcollection.asme.org/GT/proceedings-abstract/GT2019/V009T38A017/1067221

[5] F. Di Sabatino, B. J. Connolly, O. M. Pryor, and S. H. White, "Perspectives on oxy-fuel combustion for supercritical CO2 direct-fired power cycle," *Appl. Energy Combust. Sci.*, vol. 20, p. 100297, 2024.

[6] S. Gupta, S. Aithal, A. Hosangadi, T. Weathers, and J. Fetvedt, “Development of a Laser Igniter for Direct Fired sCO2 Combustor,” in *Turbo Expo: Power for Land, Sea, and Air*, American Society of Mechanical Engineers, 2022, p. V009T28A014. Accessed: Jan. 09, 2024. [Online]. Available: https://asmedigitalcollection.asme.org/GT/proceedings-abstract/GT2022/V009T28A014/1149220
[7] P. A. Strakey, “Oxy-combustion modeling for direct-fired supercritical CO2 power cycles,” *J. Energy Resour. Technol.*, vol. 141, no. 7, p. 070706, 2019.
[8] S. White, G. Berry, and B. Connolly, “Design of a 1MW Direct-Fired Oxy Combustor for sCO2 Power Cycles,” in *Turbo Expo: Power for Land, Sea, and Air*, American Society of Mechanical Engineers, 2022, p. V009T28A007. Accessed: Jan. 11, 2024. [Online]. Available: https://asmedigitalcollection.asme.org/GT/proceedings-abstract/GT2022/V009T28A007/1149234
[9] D. T. Banuti, L. Shunn, S. Bose, and D. Kim, “Large eddy simulations of oxy-fuel combustors for direct-fired supercritical CO2 power cycles,” in *The 6th International Symposium on Supercritical CO2 Power Cycles*, 2018. Accessed: Jan. 11, 2024. [Online]. Available: https://sco2symposium.com/papers2018/oxy-combustion/149_Pres.pdf
[10] D. Cecere, E. Giacomazzi, and N. M. Arcidiacono, “DNS of a non-premixed CH4/O2 flame in a supercritical CO2 environment,” *Fuel*, vol. 362, p. 130709, 2024.
[11] G. Indelicato *et al.*, “Numerical Investigation of High Pressure CO $_2$ -Diluted Combustion Using a Flamelet-based Approach,” *Combust. Sci. Technol.*, vol. 192, no. 11, pp. 2028–2049, Nov. 2020, doi: 10.1080/00102202.2020.1811243.
[12] S. Suzuki, Y. Iwai, M. Itoh, Y. Morisawa, P. Jain, and Y. Kobayashi, “High pressure combustion test of gas turbine combustor for 50MWth supercritical CO2 demonstration power plant on Allam cycle,” in *Proceedings of the International Gas Turbine Congress*, International Gas Turbine Congress Tokyo, Japan, 2019, p. 232. Accessed: Jan. 11, 2024. [Online]. Available: https://www.researchgate.net/profile/Parikshit-Jain/publication/338431114_Supercritical_CO2_Demonstration_Power_Plant_on_Allam_Cycle/links/5e66c2424585153fb3d1be8e/Supercritical-CO2-Demonstration-Power-Plant-on-Allam-Cycle.pdf
[13] M. Bukar, S. Basnet, T. KIm, and G. Magnotti, “Effect of O $_2$ /CO $_2$ ratio on stability and near field structure of oxyfuel jet diffusion flames at atmospheric pressure.,” in *AIAA SCITECH 2022 Forum*, San Diego, CA & Virtual: American Institute of Aeronautics and Astronautics, Jan. 2022. doi: 10.2514/6.2022-0640.
[14] M. Bukar, S. Basnet, T. Kim, W. L. Roberts, and G. Magnotti, “Pressure effects on soot formation in turbulent CH4 flames in an O2/CO2 atmosphere,” *Fuel*, vol. 406, p. 136895, 2026.
[15] J. Yang, Y. Gong, Q. Guo, H. Zhu, L. He, and G. Yu, “Dilution effects of N2 and CO2 on flame structure and reaction characteristics in CH4/O2 flames,” *Exp. Therm. Fluid Sci.*, vol. 108, pp. 16–24, 2019.
[16] P. Kutne, B. K. Kapadia, W. Meier, and M. Aigner, “Experimental analysis of the combustion behaviour of oxyfuel flames in a gas turbine model combustor,” *Proc. Combust. Inst.*, vol. 33, no. 2, pp. 3383–3390, 2011.
[17] P. Glarborg and L. L. B. Bentzen, “Chemical Effects of a High CO $_2$ Concentration in Oxy-Fuel Combustion of Methane,” *Energy Fuels*, vol. 22, no. 1, pp. 291–296, Jan. 2008, doi: 10.1021/ef7005854.
[18] C. Y. Liu, G. Chen, N. Sipöcz, M. Assadi, and X.-S. Bai, “Characteristics of oxy-fuel combustion in gas turbines,” *Appl. Energy*, vol. 89, no. 1, pp. 387–394, 2012.
[19] A. N. Mazas, D. A. Lacoste, and T. Schuller, “Experimental and numerical investigation on the laminar flame speed of CH4/O2 mixtures diluted with CO2 and H2O,” in *Turbo Expo: Power for Land, Sea, and Air*, 2010, pp. 411–421. Accessed: Jan. 11, 2024. [Online]. Available: https://asmedigitalcollection.asme.org/GT/proceedings-abstract/GT2010/411/339240
[20] J. R. Serrano, J. Martín, J. Gómez-Soriano, and R. Raggi, “Theoretical and experimental evaluation of the spark-ignition premixed oxy-fuel combustion concept for future CO2 captive powerplants,” *Energy Convers. Manag.*, vol. 244, p. 114498, 2021.
[21] R. K. Rahman *et al.*, “Probing the effects of NOx and SOx impurities on oxy-fuel combustion in supercritical CO2: Shock tube experiments and chemical kinetic modeling,” *J. Energy Resour. Technol.*, vol. 142, no. 12, p. 122302, 2020.
[22] J. Lee, G. J. Hwang, J. I. Lee, A. Jamal, and N. I. Kim, “Flame stabilization and soot emission of methane jet flames for CO2 diluted oxy-combustion at elevated pressure,” *Combust. Flame*, vol. 231, p. 111490, 2021.

[23] F. Di Sabatino, B. Connolly, K. Partridge, and S. White, “EXPERIMENTAL INVESTIGATION ON LASER IGNITION AND FLAME STABILIZATION IN AN OXYGEN/METHANE CO2-DILUTED COMBUSTOR AT ELEVATED PRESSURES,” vol. Turbo Expo: Power for Land, Sea, and Air, 2024.

[24] N. Level Otsu, “A threshold selection method from gray-level histogram,” *IEEE Trans Syst Man Cybern*, vol. 9, no. 1, pp. 62–66, 1979.

ACKNOWLEDGEMENTS

This work was supported by Mitsui Energy Development CO., LTD. under Southwest Research Institute contract n^{o} 18-101647. The authors would like to thank Mr. Joshua Arguello, Mr. James Donnelly, and Mr. John Stubbs for their support in assembly and making the combustor operable.